

## **Productivity controls on the redox variation in the southeastern Arabian Sea sediments during the past 18 kyr**

**J.N. Pattan, G. Parthiban\*, Ankeeta Amonkar**

CSIR-National Institute of Oceanography, Dona Paula, 403 004, Goa, India

Corresponding author, \*parthi@nio.org

phone: 91-832-2450461

### **Abstract**

Redox-sensitive elements (uranium, molybdenum and cadmium) and productivity proxies (total organic carbon, calcium carbonate and phosphorous) were analysed to assess the importance of productivity on redox variation for the last ~18 kyr in a sediment core off Cochin at a water depth of 280 m in the southeastern Arabian Sea. These proxies document a combination of higher productivity and intense suboxic conditions during the last deglaciation (~18 to 13 kyr) and late Holocene (5.5 kyr to Present) versus lower productivity and less suboxic conditions between these intervals (~13 to 5.5 kyr). The productivity and redox proxies behave similar to one another suggesting that the variations in productivity controlled the redox conditions. This relationship is supported by patterns during the last deglaciation, when a decrease in productivity at ~16 kyr preceded improved deep water oxygenation by ~14 kyr. Therefore, productivity changes were responsible for the development of reducing conditions in shallow waters in the southeastern Arabian Sea.

**Keywords:** sediments, redox-sensitive elements, productivity proxies, redox conditions, last deglaciation, late Holocene.

## 1. Introduction

The Arabian Sea, in the northern Indian Ocean is a relatively small but biogeochemically an active area of the world oceans (Owen et al. 1991; Gage et al. 2000). The Arabian Sea is unique due to its northern part being land locked, inflow of major rivers such as the Indus which delivers abundant terrigenous material and effects the monsoon dynamics. The Arabian Sea experiences southwest monsoon (June-September) and northeast monsoon (November-February). The seasonal reversal of winds leads to strong upwelling of nutrient-rich water from the deeper depths along the continental shelf of India resulting in high surface productivity and high export particle flux from the euphotic zone during southwest monsoon (Qasim, 1982; Nair et al. 1989). The Arabian Sea receives very high carbonate fluxes (over  $300 \text{ mg m}^{-2} \text{ day}^{-1}$ ) that are mainly contributed by foraminifers, and coccolithophorids with minor contribution from pteropods, and high opal fluxes (above  $100 \text{ mg m}^{-2} \text{ day}^{-1}$ ) contributed by diatoms, radiolarians and silicoflagellates during southwest monsoons (Nair et al. 1989; Ramaswamy and Nair, 1994). Similarly, organic carbon fluxes and lithogenic fluxes were also high during SW monsoons (Nair et al. 1989; Haake et al. 1992). The northern Arabian Sea is characterized by a pronounced mid-water oxygen minimum zone (OMZ) with oxygen concentration reaching as low as  $< 0.05 \text{ ml L}^{-1}$  between water depths of 150 and 1250 m (Wyrcki, 1973; Naqvi, 1991; Reichert et al. 2002). This intense OMZ results from high annual organic particle fluxes and moderate thermohaline ventilation. Earlier, northwest off Oman margin, (Gage et al. 2000) and northeastern Pakistan margin (Cowie and Levin, 2009), parts of Arabian Sea have been studied extensively for benthic process like morphology, diversity and taxonomy of foraminifers, bioturbation, sediment geotechnical characteristics, nature of organic matter, biogeochemical and aerobic, suboxic and anaerobic microbial process. However, such a study for the southeastern Arabian Sea has been lacking.

Reconstruction of the past oxygenation conditions in marine sediments can be studied with the help of proxies such as redox-sensitive elemental concentration, laminations and foraminifer species assemblages which in turn help to understand different depositional environments (Wignall, 1994; Tribovillard et al. 2006; Calvert and Pedersen 2007; Algeo and Tribovillard, 2009; Algeo et al. 2012). These proxies further help to detect changes in export production and modification in ventilation through bottom currents (Crusius et al. 2004; Ivanochko and Pedersen 2004; Nameroff et al. 2004; McKay et al. 2005; Dean et al. 2007; Chang et al. 2014; Salvattecchi et al. 2016). Redox-sensitive elements such as Mn, Fe, U, Mo and Cd have different solubility under different redox conditions and their enrichment or depletion in the sediments compared to shale is used to trace the development of oxic, suboxic and anoxic conditions at or close to sediment-water interface

(McManus et al. 2006; Francoise-Elbaz-Poulichet et al. 2014). Mn and Fe are generally enriched in sediments overlain by the oxygenated bottom waters, whereas they are depleted in sediments formed below suboxic bottom waters (Calvert and Pedersen, 1993; 2007). Uranium accumulates in marine sediments under the suboxic or anoxic (absence of oxygen and hydrogen sulfide) conditions whereas Mo and Cd enrichment occurs as insoluble sulfides in the presence of hydrogen sulfide (Rosenthal et al. 1995; Helz et al. 1996; Erickson and Helz 2000; Zheng et al. 2000). However, Mo is also enriched under oxic conditions concurrently with the formation of Mn oxyhydroxides phase with a nearly constant ratio of Mo/Mn of 0.002 (Shimmield and Price 1986).

Changes in the redox-conditions can also develop ~~ocean~~ due to increased sedimentation rate and corresponding decreased oxygen flux, increased carbon flux, due to higher export productivity and decreased ventilation of bottom waters (McKay et al. 2005). It is important to know the intensity of each factor responsible for the development of reducing conditions. Studies related to paleoredox-conditions in the southeastern Arabian Sea are sparse (Sarkar et al. 1993; Pattan and Pearce, 2009) and are for only deep water locations (~2500 m) of southeastern Arabian Sea. It was suggested that development of suboxic conditions was mainly due to the poorly ventilated Southern Ocean deep waters particularly during the Last Glacial Maximum. Recently, Pattan et al (2017) studied sediment cores from the OMZ off Goa, in the eastern Arabian Sea and reported intense reducing conditions caused by ventilation during the last deglaciation and Heinrich events (H1,H2,H3). There are a number of studies related to early diagenesis, redox state and ventilation in the northeast and northwest part of Arabian Sea (van der Weijden et al. 1999., 2006; Suthhof et al. 2001; Altabet et al. 2002; Reichart et al. 2004; Pichevin et al. 2007; Boning et al. 2009; Luckge et al. 2012). But there is virtually no information on the factors controlling the development of paleoredox conditions at shallow water depth (< 500 m) in the southeastern Arabian Sea. Therefore, in the present study, redox-sensitive elements and productivity proxies were studied in order to understand the relation between export productivity and development of sedimentary redox conditions during the past 18 kyr in the southeastern Arabian Sea.

## **2. Material and Methods**

A 3.33 m long sediment gravity core (GC-05) was retrieved during August-September 1994 onboard *A. A. Sidernko* (AAS-VI/GC-05) off Cochin (Lat: 10<sup>o</sup>.22` N; Long: 75<sup>o</sup> 33`E) from the southeastern Arabian Sea at a water depth of 280 m (Fig.1a & b). The upper 0.5 m of the core is olive grey (5Y 3/2), silty clay and the remainder is olive black (5Y 2/1) clayey silt (Thamban et al. 2002). Within the sediment core few pteropods and small gastropod shells were noticed at ~ 0.8 m, 1.5 m and 3.1 m and there were no signs of laminations or bioturbation in the sediment core.

The sediment core was sub-sampled at 5 cm interval, oven dried and finely powdered in an agate mortar. For the chemical analysis, 50 mg of sediment was treated with 10 ml of suprapur (Merck®) acid mixture of HF+ HNO<sub>3</sub> + HClO<sub>4</sub> (7:3:1) and heated on a hot plate until it was pasty. To ensure complete dissolution one more cycle of the same acid mixture was added and digested. Later, 4 ml of 1:1 HNO<sub>3</sub> (1 volume of HNO<sub>3</sub> and 1 volume of water) was added, then heated for 5 minutes and 1 ml of 1 ppm h added as an internal standard and final volume was made to 100 ml with ultra pure water (18.2 MΩ). Similarly, a standard reference material (MAG-1), blanks and duplicate samples were also digested. These solutions were analysed for a few major, minor and trace elements using an Inductively Coupled Plasma- Mass Spectrometer (Thermo X-Series II) at the National Institute of Oceanography, Goa. The accuracy of the data set based on a standard reference material and precision based on duplicate analysis were better than ± 7%. Total organic carbon data were used from Thamban et al. (2001). Calcium carbonate content was calculated based on calcium content as determined by ICP-MS and later the detrital Ca {K<sub>sample</sub> \* (Ca/K)<sub>ucc</sub>} was subtracted from it. Calcium carbonate values are slightly lower than earlier estimated by gasometric technique (Thamban et al. 2001). However, its distribution pattern remains very similar to one another.

The chronostratigraphy of the sediment core is based on five AMS <sup>14</sup>C dates on *Globigerinoides sacculifer* (250-500 μm size fraction) and stable isotope measurements were carried out at the Isotope Laboratory, University of Bremen, Germany, using a Finnigan 252 MAT Mass Spectrometer attached with an automated CO<sub>2</sub> preparation Unit (Thamban et al. 2001). Age-depth model presented in Fig. 2a was based on AMS dates and extrapolated for the entire core depth. The calculated sedimentation rates (cm/kyr) were shown in Fig.2b. Dry bulk densities (DBD) were calculated using a non-linear regression equation developed for the Indian Ocean by Clemens et al. (1987) based on the calcium carbonate content of bulk sediment (Fig. 2c).

$$DBD = 3.104 \times 10^{-5} (\text{CaCO}_3 \%)^2 + 2.176 \times 10^{-3} (\text{CaCO}_3 \%) + 0.430 \text{ -----1}$$

Bulk accumulation rates (g/cm<sup>2</sup>/ka) were estimated by using linear sedimentation rate and DBD (Fig.2d). Element fluxes (g/cm<sup>2</sup>/kyr) were calculated by using linear sedimentation rates, DBD and individual element concentration.

Enrichment Factor (EF) was obtained using the equation of Barbieri et al, (2016).

$$EF = (\text{Metal/Al})_{\text{sample}} / (\text{Metal/Al})_{\text{shale}} \text{ -----2}$$

Grain size analysis of the sediment core was carried out by Thamban et al. (2001) following standard procedure (Folk, 1968).

### 3. Results

#### 3.1. Sedimentation rate, dry bulk density, bulk accumulation rate, and grain size

The age-core depth model for the sediment core suggests that sedimentation rates vary from 6 to 51 cm/kyr being highest (21 to 51 cm/kyr) during the last deglaciation (~18 to 13 kyr) and late Holocene i.e last 5.5 kyr (16 to 20 cm/kyr) and lowest (6 cm/kyr) from 13 to 5.5 kyr (Fig. 2b). The DBD was high (0.525 to 0.5 g/cm<sup>3</sup>) during the last deglaciation and late Holocene but reached a minimum of 0.425 g/cm<sup>3</sup> from ~ 13 to 5.5 kyr (Fig. 2c). Bulk accumulation rates (BAR) are highest during the last deglaciation (~25 g/cm<sup>2</sup>/kyr) and reduced to ~8 to 10 g/cm<sup>2</sup>/kyr during late Holocene and reached a minimum of ~ 2 g/cm<sup>2</sup>/kyr between 13 and 5.5 kyr (Fig. 2d). Sand content was lowest (1 to 22 wt%) followed by an increase in silt (26 to 55 wt%) and highest clay content (30 to 70 wt% Fig. 3a). Sand and silt contents were highest during the last deglaciation and late Holocene and lowest from 13 to 5.5 kyr. On the contrary, clay content was highest (~ 70 wt%) from 13 to 5.5 kyr and comparatively low (30- 40 wt%) during last deglaciation and late Holocene (Fig.3a).

#### 3.2. Elemental concentrations and ratios

Titanium (Ti) is a representative element of detrital source and varies from 0.37 % to 0.8 % with an average of 0.54 % (Fig. 3b). Ti content was low during the last deglaciation (0.52 %) and late Holocene (0.41 %) but reached a distinct high (0.69 %) during 13 to 5.5 kyr. Titanium flux follows similar trend of bulk Ti content (Fig.3b). Total organic carbon (TOC) content ranges from 1.3 to 3.8 % with high values during late Holocene (2.5 to 3.8 %) and low of 1 to 1.5 % in the rest of the core. (Fig. 3c). The C<sub>org</sub>:P (molar ratio) in the sediment core varies from ~40 to 120 being highest during late Holocene (Fig. 3c). Calcium carbonate is one of the productivity proxies and shows large variations ranging from 4 to 31 % with high carbonate during the last deglaciation and late Holocene but low during 13 to 5.5 kyr (Fig. 4a). Calcium carbonate flux (g/cm<sup>2</sup>/kyr) varies from 0.2 to 7 and follows bulk carbonate trend (Fig 4a). Organic carbon flux varies from 0.1 to 0.42 being highest during the last deglaciation and late Holocene (Fig.4b). Phosphorous content does not vary much (0.06 to 0.15 %) (Fig. 4c), whereas, its fluxes reaches high during the last deglaciation and late Holocene (Fig 4c).

The mean concentration of Mn, Fe, Mo, U and Cd in the sediment core is 369 ppm, 4.79 %, 3.52 ppm, 6.56 ppm and 1.44 ppm, respectively. The Mn/Al, ratio varies from 30 to 70 X 10<sup>-4</sup> and is lower than the shale (Fig. 5a). In comparison, the Fe/Al ratio varies from 0.44 to 0.8 which is higher than shale (Fig. 5b; Taylor and McLennan, 1985). Highest Mo/Al ratio of up to ~ 1.5 X 10<sup>-4</sup> are recorded during the last deglaciation and late Holocene (Fig.5c). High U/Th ratios up to 1.1 occurs

during late Holocene (Fig. 5d). The Cd/Al ratio is high during the last deglaciation and late Holocene (Fig. 5e). The element fluxes of Mn, Fe, Mo, U and Cd are shown in Fig. 5a, b, c, d & e respectively.

## 4. Discussion

### 4.1 Variation in productivity and terrigenous matter since 18 kyr

The distribution patterns of productivity proxies such as CaCO<sub>3</sub>, TOC, and P and their respective fluxes are similar over the last 18 kyr (Fig. 4a, b & c). These productivity proxies were high during the last deglaciation and late Holocene, but low between ~13 and 5.5 kyr (Fig. 4a, b & c). These proxies and their flux suggest high productivity during the last deglaciation and late Holocene but low during ~13 to 5.5 kyr (Fig. 4a). On the other hand, Ti a terrigenously sourced element behaves contrary to that of calcium carbonate as expected (Fig. 3 & 4). Ti content and its flux (Fig. 3b) were low during the last deglaciation and late Holocene and highest from ~13 to 5.5 kyr suggesting intensification of the southwest monsoon which would have increased fresh water runoff and terrigenous sediment flux. On the contrary, the southwest monsoon was relatively weak during the last deglaciation and late Holocene. The increased monsoonal precipitation started at ~13.5 ka and is close to the earlier observation made based on  $\delta^{18}\text{O}$  fluctuations and clay mineral assemblages at ~15.2 ka in the southeastern Arabian Sea (Thamban et al. 2001; 2002), at ~13.8 ka based on the peat records from Nilgiri hills, India (Sukumar et al. 1993) and at ~15 ka from paleo-drainage records (Mishra, 2000). The intense monsoonal precipitation in the present sediment core location continued up to 4 kyr and became weaker from 4 to 2 kyr and stabilized during the last 2 kyr.

Phosphorous (P) can be delivered to the sediments mainly in association with organic matter and therefore P content can be used as a productivity proxy (Delaney 1998). During degradation of the organic matter, P is released to interstitial waters and subsequently adsorbed on to grain surfaces, bound to Fe-oxyhydroxides and diffused back to bottom waters (Ingall et al. 1993; Babu and Nath, 2005). High P flux during the last deglaciation and late Holocene suggest high productivity and its low flux from 13 to 5.5 kyr indicates low productivity (Fig. 4c). Interestingly, at ~16 ka paleo-productivity was comparatively low within the last deglaciation period. During the last deglaciation, however, TOC and P contents remained low and do not match with the other productivity proxies like calcium carbonate. This is indicated by a positive correlation between TOC and P ( $r = +0.82$ ;  $p < 0.001$ ,  $n = 70$ ; Table 1) and could be due to dilution i.e. high sedimentation rate during the last deglaciation (Fig. 2b). This is evident by the low C<sub>org</sub>:P molar ratio which is one of the useful paleoproductivity proxy and this ratio will be highest of 150-200 during anoxic, ~75 to 130 during

suboxic to anoxic and  $\sim 40$  during oxic to suboxic conditions (Algeo and Ingall, 2007). This ratio is highest (60-80) during late Holocene suggesting relatively less altered marine organic matter, compared to Redfield ratio of 106 and it decreased to 30 at 6 ka and reached to lowest of 20 from 18 to 6 kyr (Fig. 3c). This suggests an intense diagenesis of organic matter from 18 to 6 kyr resulting in low organic carbon content. Further, it is interesting to note that TOC and  $C_{org}$ :P molar ratio co-vary with  $\sim 10:1$  ratio from 18 to 5.5 kyr, subsequently P increased by a factor of  $\sim 2$  to 3 relative to TOC during late Holocene. This suggests that P-bearing compounds are still undergoing rapid decay process after which they mostly decay, and probably result in a constant  $C_{org}$ :P ratio.

#### 4.2. Variation in redox conditions since 18 kyr

Manganese (Mn) is a redox sensitive element and in oxic environment precipitates as  $Mn^{4+}$  whereas under suboxic environment it dissolves into pore water as  $Mn^{2+}$  and diffuses upwards to precipitate as  $Mn^{4+}$  once oxic environment is encountered (Lynn and Bonatti, 1965). Similarly Fe is also enriched in oxic conditions compared to suboxic conditions. The Mn/Al ratio ( $30$  to  $70 \times 10^{-4}$ ) is lower than the shale value of  $90 \times 10^{-4}$  (Taylor and McLennan, 1985) and comparatively low (30-50) during the late Holocene, probably indicate enhanced reducing conditions as compared to rest of the core (Fig. 5a). The Fe/Al ratio does not show any trend during the entire last 18 kyr and is always higher (0.44 to 0.8) as compared to shale value of 0.45 (Taylor and McLennan, 1985, Fig. 5b). This could be due to an additional supply of iron probably from the aeolian dust in addition to the terrigenous source (Pattan et al. 2017). A high Fe/Al ratio is also recorded from the OMZ off Goa at a water depth of 643 m and 1086 m and it appears that sediments throughout the Arabian Sea have a higher Fe/Al ratio (Pattan et al. 2011, 2017). The high Fe/Al ratio above average shale suggests that Fe reduction may be incomplete under reducing conditions and is similar to the OMZs off the Pakistan margin (Law et al. 2009) and in the northeastern Pacific Ocean (Landing and Bruland, 1987). This probably suggests supply of Fe is more than its reduction rate.

Molybdenum in the marine sediments can be enriched under sulphidic anoxic conditions by incorporating into pyrite (Ericson and Helz 2000; Zheng et al. 2000; Algeo and Maynard 2004; Algeo and Lyons 2006; Tribovillard, et al. 2008). Ericson and Helz (2000) suggested that Mo precipitation occurs when a threshold of  $11 \mu M$  of  $H_2S$  is attained. Higher Mo concentrations are also associated with Mn cycling since adsorption with Mn oxide phase can lead to elevated concentrations under oxic conditions and retaining Mo/Mn ratio always close to 0.002 (Shimmiel and Price, 1986). The mean Mo/Mn ratio of 0.01 suggests sediments from the southeastern Arabian Sea never reached oxic conditions. Mo concentration varies from 1.4 ppm to 13.5 ppm (average 3.52 ppm) and shows considerable enrichment compared to shale value of  $\sim 1.0$  ppm (Taylor and

McLennan, 1985). The high Mo/Al ratio during the last deglaciation and late Holocene suggests suboxic conditions and it reached lowest during ~13 to 5.5 kyr which points to reduced suboxic condition (Fig. 5c). The Mo concentration (mean 3.52 ppm) in the present sediment core is lower than the Black Sea or Cariaco Trench (20 to 60 ppm) which are typical anoxic basins (Emerson and Husted, 1991; Crusius et al. 1996), sediments deposited under OMZ of Oman (2-23 ppm; Shimmiel, 1992) and Indian margins (up to 30 ppm; Sirocko, 1995) suggest that the intensity of suboxic condition was lower in the present core location. On the contrary, Mo content is higher than in the sediments of equatorial Indian Ocean (0.7 ppm: Pailler et al. 2002) and deep southeastern Arabian Sea (~ 1 ppm: Pattan and Pearce, 2009) reflecting relatively higher suboxic conditions.

In oxic environment, generally U is present as soluble U(VI) and is chemically unreactive (Calvert and Pedersen, 1993), while under reducing conditions U (VI) is reduced to U(IV) which is less soluble, becomes more particle reactive and is subsequently adsorbed onto the sediment or clay mineral surfaces (Mangini, 1978; Barnes and Cochran, 1990; Klinkhammer and Palmer, 1991; Tribovillard et al. 2005). Uranium content varies from 2.86 ppm to 13.4 ppm and is higher than earlier reported (3.6 ppm to 8.1 ppm) within the OMZ at a water depth of 218 to 325 m in the eastern Arabian Sea (Nath et al. 1997) and also from the deep sea (2500 m) sediment core of the southeastern Arabian Sea (Pattan and Pearce, 2009). It is significantly lower than as reported in the OMZ off Goa at a water depth of 643 m (5 to 23 ppm with an average of 10 ppm) and 1083 m (6 to 17 ppm with an average of 11 ppm; Pattan et al. 2017). The U/Th ratio is highest in late Holocene (up to 1) and is reduced to 0.3 to 0.4 during the last deglaciation (Fig. 5d). On the contrary, U/Th ratio is just above shale value of 0.21 during ~14 to 5.5 kyr (Fig. 5d). This suggests suboxic conditions during late Holocene and last deglaciation. The deep southeastern Arabian Sea off Cochin (2500 m) has U/Th ratio of ~0.25 during the Holocene which is contrary to the present study (Pattan and Pearce, 2009).

Cadmium has a single oxidation state ( $Cd^{2+}$ ) and its authigenic enrichment require reducing conditions and also needs nanomolar levels of hydrogen sulfide (Rosenthal et al. 1995; van Geen et al. 1995; Kuwabara et al. 1999). Similar to U and Mo distribution, Cd is also enriched (0.12 to 3.3 ppm) in the present sediment core compared to shale /upper continental crustal value (~0.1 ppm) (Taylor and McLennan, 1985). The Cd/Al ratio varies from 0.1 to  $0.55 \times 10^{-4}$  and high during the last deglaciation and late Holocene suggest suboxic conditions. On the contrary, low Cd/Al ratio of  $0.11 \times 10^{-4}$  from ~13 to 5.5 kyr is an indicative of less suboxic conditions (Fig. 5e).



The temporal trends of fluxes of Mn, Fe, Mo, U and Cd are distinctly highest during the last interglacial and late Holocene (intense suboxic ) but reached minimum from ~13 to 5.5 kyr (less suboxic) and their distribution patterns are very similar to each other (Fig. 5a, b, c, d & e).

The concentration of redox-sensitive elements and biological productivity proxy together document intense suboxic conditions during the last deglaciation and late Holocene whereas, low productivity and low concentrations of redox-sensitive elements from ~13 to 5.5 kyr indicates less suboxic conditions (Fig. 4 & 5). The slight decrease in the productivity within the last deglaciation (~ 16 ka) is not reflected in the distribution of U/Th and Cd/Al whereas Mo/Al shows increased value suggesting more reducing conditions and this was preceded and enhanced by deep water oxygenation by ~ 14 ka.

It is evident that  $\text{CaCO}_3$  TOC and P contents (productivity proxies) are highest during the last deglaciation compared to late Holocene and behave very similar to sedimentation rate, BAR, fluxes of Mn, Fe, UMo, U and Cd and metal ratios of Mo/Al, U/Th and Cd/Al. These factors probably suggest that productivity is controlled by the high sedimentation rate and BAR during the last deglaciation, and were responsible for changes in redox conditions. This may suggest that during the last deglaciation and late Holocene  $\text{H}_2\text{S}$  chemocline resulted in the sediment that migrated upwards towards the sediment-water interface because of reduced sediment ventilation. Therefore, faster sedimentation results in a shallow chemocline i.e intense suboxic conditions. Slow sedimentation rate from ~13 to 5.5 kyr which allowed oxygen to penetrate more deeply into the sediment resulted in a comparatively less suboxic conditions at the sediment-water interface. It is interesting to note that during the last deglaciation, sea level was lower by ~ 100 m compared to Present day (Fig. 1c; Hashimi et al. 1995). As a result during the last deglaciation, more terrigenous material might have been supplied in the present sediment core location. This caused high sedimentation rate (Fig. 2b), BAR (Fig. 2d) and increased productivity (Fig 4).

#### *4.3. Controls on redox variation since 18 kyr*

Redox conditions in the marine environment are generally controlled by productivity or ventilation and vary from region to region. In the present sediment core, at a shallow water depth (280 m), productivity was high during the last deglaciation and late Holocene and low from ~13 to 5.5 kyr. Some of the productivity proxies are well correlated with the redox-sensitive elements (Table 1) and suggestive of suboxic conditions. The low productivity from ~ 13 to 5.5 kyr resulted in a less suboxic depositional conditions. Among the last deglaciation and late Holocene, suboxic condition was more intense during former compared to latter period. This is mainly due to high

sedimentation rate during the last deglaciation compared to late Holocene which resulted in high productivity and in turn development of intense suboxic conditions. Ivanochko and Pedersen, 2004; and Cartapanis et al. 2011 suggested the absence of any correlation between total organic carbon with Mo or U in the sediments and that ventilation was more effective rather than the productivity changes. Correlation matrix between productivity proxies (CaCO<sub>3</sub>, TOC and P) and redox-sensitive elements (U, Mo and Cd) are presented in Table 1. In the present sediment core, there is a strong positive correlation between TOC and U ( $r=0.93$ ,  $p(a) < 0.001$ ,  $n=70$ ),) whereas, a weak positive correlation between TOC and Mo ( $r = 0.38$ ,  $p(a) < 0.001$ ,  $n=70$ ) is observed (Table 1; Fig. 6a & b) and is indicative of productivity controlled the development of reducing conditions in the shallow sediments of southeastern Arabian Sea during the last 18 kyr. High surface productivity caused by the strong upwelling due to seasonal reversal of winds in the continental shelf of India was reported earlier (Qasim, 1982; Nair et a., 1989). Recently, Pattan et al. (2017) did not notice any relationship between TOC with U or Mo in the sediments from OMZ off Goa at 642 and 1086 m water depth of eastern Arabian Sea, suggesting that ventilation control the reducing conditions. This is in contrast with present study where development of suboxic condition was controlled by the productivity.

#### 4.4. Enrichment factor (EF) of U and Mo and Mo/U<sub>auth</sub>

In low oxygen marine system, Mo-U co-variation patterns have potential to provide insights regarding bottom water redox conditions and paleoceanographic processes (Algeo and Tribovillard 2009; Tribovillard et al., 2012). In the marine sediments Mo-U enrichment factors and authigenic enrichments are minor or close to 1 under oxic environment, modest EFs of  $< 10$  in suboxic environment where U-EF greater than Mo-EF and  $> 10$  is indicative of anoxic to euxinic depositional conditions processes (Algeo and Tribovillard 2009; Tribovillard et al., 2012). The behaviors of U and Mo-EFs during the last 18 kyr are shown in (Fig. 7). The U-EF and Mo-EF reaches up to 5 and 6 during the last 18 kyr respectivel suggesting suboxic depositional conditions (Algeo and Tribovillard 2009; Tribovillard et al., 2012). The Mo-EFs are greater than U-EFs during the early last deglaciation (~18 to 15.5 kyr) whereas during the late last deglaciation (15.5 to 14 kyr) U-EFs are greater than Mo-EFs. Between ~13 to 5.5 kyr both U and Mo -EFs remains low, but among them U-EFs are slightly greater than Mo-EFs. This is mainly due to differential geochemical behavior of U and Mo; where uptake of authigenic U by marine sediments begins at the Fe (II) – Fe (III) redox boundary and authigenic Mo enrichment requires presence of H<sub>2</sub>S. In the last 2 kyr U-EFs are greater than Mo-EFs though it is under intense suboxic conditions. The 13 to 5.5 kyr interval represents comparatively less suboxic conditions and is supported by the highest Mn/Al ratio (Fig. 5a). The last deglaciation and late Holocene are associated with suboxic conditions, where Mo enrichment is seen

(although Mo enrichment is modest) which is possible under presence of little H<sub>2</sub>S at the sediment-water interface.

Marine sediments under suboxic conditions result in modest Mo and U enrichments and (Mo/U)<sub>auth</sub> ratios lower than seawater ratio, whereas anoxic conditions result in strong Mo and U enrichment associated with higher (Mo/U)<sub>auth</sub> ratio as total authigenic concentration increases (McManus et al. 2006; Algeo and Tribovillard, 2009; Scholz et al. 2011). The Mo/U<sub>auth</sub> ratio of < 3.2 and > 3.2 suggests suboxic and sulfidic conditions respectively (Algeo and Tribovillard, 2009; Salvattecchi et al. 2016). In the present sediment core, (Mo/U)<sub>auth</sub> ratio is < 3.2 suggesting suboxic conditions (Fig. 8a) rather than sulfidic environment. The last deglaciation has comparatively higher (Mo/U)<sub>auth</sub> than late Holocene reflecting that the former had intense suboxic conditions compared to the latter (Fig. 8a). This is further supported by the cross plot of Mo-EF versus U-EF (Fig. 8b) where all the sediments occupy suboxic field of unrestricted marine and also on 0.3 x SW line which is again indicative of suboxic depositional conditions (Algeo and Tribovillard, 2009; Tribovillard et al., 2012; Salvattecchi et al. 2016). Uranium-Mo EFs and (Mo/U)<sub>auth</sub> suggest that the sediments during the last 18 kyr in the southeastern Arabian Sea never reached sulfidic conditions but remained under suboxic depositional environment.

## 5. Conclusions

- Productivity was high during the last deglaciation, late Holocene and low between 13 and 5.5 kyr. On the contrary, supply of terrigenous material was high from 13 to 5.5 kyr and low during the last deglaciation and late Holocene. This suggests that southwest monsoon was intense from 13 to 5.5 kyr resulting in an increase of fresh water run-off and terrigenous sediment flux to southeastern Arabian Sea and was weak during the last deglaciation and late Holocene.
- Higher productivity resulted in an intense suboxic conditions during the last deglaciation and late Holocene. The time period between 13 and 5.5 kyr was comparatively under less suboxic conditions and was associated with less productivity. This indicates that the development of suboxic conditions were mainly controlled by the productivity changes at shallow waters of the southeastern Arabian Sea.
- The enrichment factors of U and Mo and (Mo/U)<sub>auth</sub> suggest that the sediments never reached sulfidic but remained in the suboxic depositional conditions during the last 18 kyr in the southeastern Arabian Sea

## Acknowledgements

Authors are grateful to Prof. Thomas J. Algeo, University of Cincinnati, USA and an anonymous reviewer for their valuable suggestions and critical comments which helped us to improve the quality of the manuscript. Special thanks to anonymous reviewer for his very detailed editing of the manuscript, in addition to his valuable suggestions. Authors wish to thank Director, National Institute of Oceanography, Goa, India for the support to carry out this work, Dr. S. D. Iyer, Dr. S. M. Karisiddaih for their editorial suggestions and Chief Editor, Quaternary International journal for his encouragement, This is NIO contribution No. -----

## References

- Algeo, T.J. Maynard, J.B., 2004. Trace element behavior and redox facies in core shales of upper Pennsylvanian Kanas-type cyclotherms. *Chemical Geology* .206, .289-318.
- Algeo, T.J., Lyons, T.W., 2006. Mo-total organic carbon covariation in modern anoxic marine environments: implications for analysis of paleoredox and paleohydrographic conditions. *Paleocenography* 21, doi.1010.1029. 2004PA001112
- Algeo, T.J., Ingall, E., 2007. Sedimentary C<sub>org</sub>: P ratios, paleo-ocean ventilation and Phanerozoic atmospheric pCO<sub>2</sub>. *Paleogeography Paleoclimatology Paleoecology*. 256, 130-155.
- Algeo, T.J., Tribouillard, N., 2009. Environmental analysis of paleoceanographic systems based on molybdenum –uranium covariation. *Chemical Geology* 268, 211-225.
- Algeo, T.J., Morford, J., Cruse, A., 2012. New applications of trace metals as proxies in marine environments. *Chemical Geology* 324-325, 1-5.
- Altabet, M.A., Higginson, M.J., Murray, D.W., 2002. The effect of millennial-scale changes in Arabian Sea denitrification on atmospheric CO<sub>2</sub>. *Nature* 415 (6868), 159-162.
- Babu, C.P., Nath, B.N., 2005. Processes controlling forms of phosphorus in surficial sediments from the eastern Arabian sea impinged by varying bottom water oxygenation conditions. *Deep-Sea Research II* 52, 1865-1980.
- Barbieri M, J., 2016. The Importance of Enrichment Factor (EF) and Geoaccumulation Index (Igeo) to Evaluate the Soil Contamination. *Geology Geophysics* 2016, 5:1. <http://dx.doi.org/10.4172/2381-8719.1000237>
- Barnes, C.E., Cochran, J.K., 1990. Uranium removal in oceanic sediments and oceanic U balance. *Earth and Planetary Science Letters* 97, 94-101.
- Bonning, P., Bird, E., 2009. Millennial/centennial-scale thermohaline ventilation changes in the Indian Ocean as reflected by aragonite preservation and geochemical variations in Arabian Sea sediments. *Geochimica Cosmochimica Acta* 73, 6771-6788.
- Calvert, S.E., Pedersen, T.F., 1993. Geochemistry of Recent oxic and anoxic sediments: Implications for the geological record. *Marine Geology* 113, 67-88.

- Calvert, S.E., Pedersen, T.F., 2007. Elemental proxies for paleoclimatic and paleoceanographic variability in marine sediments: interpretations and application. In: Hillaire-Marcel, C., Vernal, A.D. (Eds), *Proxies in Late Cenozoic. Paleoceanography*, Elsevier, Amsterdam
- Cartapanis, O.K., Tachikawa, K., Bard, E., 2011. Northeastern Pacific oxygen minimum zone variability over the past 70 kyr: Impact of biological and oceanic ventilation. *Paleoceanography* 26, PA4208, doi:10.1029/2011 PA002126.
- Chang, A.S., Pedersen, T.F., Hendy, I.L., 2014. Effects of productivity, glaciation, and ventilation on late Quaternary sedimentary redox and trace element accumulation on the Vancouver Island margin, western Canada, *Paleoceanography* 29, 730–746, doi:10.1002/2013PA002581
- Clemens, S.C., Prell, W.L., Howard, W.R., 1987. Retrospective dry bulk density estimates from southeast Indian Ocean sediments- comparison of water loss and chloride –ion methods. *Marine Geology* 76, 57-69.
- Cowie, G.L, Levin, L.A. 2009. Benthic biological and biogeochemical patterns and processes across an oxygen minimum zone (Pakistan margin, NE Arabian Sea), Edited by Cowie, G.L, and Levin, L.A, *Deep-Sea Research II* 56, 261-270.
- Crusius, J., Calvert, S., Pedersen, T., Sage, D., 1996. Rhenium and molybdenum enrichments in sediments as indicators of oxic, suboxic and sulfidic conditions of deposition. *Earth Planetary Science Letters* 145. 65-78.
- Crusius, J., T. F. Pedersen, S. Kienast, L. Keigwin, and L. Labeyrie., 2004. Influence of northwest Pacific productivity on North Pacific Intermediate Water oxygen concentrations during the Bølling-Allerød interval (14.7–12.9 ka), *Geology* 32, 633–636, doi:10.1130/G20508.1
- Dean, W. E., Zheng, Y., Ortiz, J.D., van Geen, A., 2006. Sediment Cd and Mo accumulation in the oxygen-minimum zone off western Baja California linked to global climate over the past 52 kyr, *Paleoceanography* 21, PA4209, doi:10.1029/2005PA001239
- Delaney, M.L., 1998. Phosphorus accumulation in marine sediments and the oceanic phosphorus cycle. *Global Biogeochemical Cycles* 12, 563–572.
- Emerson, S.R., Husted, S.S., 1991. Ocean anoxia and the concentrations of molybdenum and vanadium in seawater. *Marine Chemistry* 34, 177-196.
- Erickson, B.E. and Helz, G.R., 2000. Molybdenum (VI) speciation in sulfidic waters: stability and liability of thiomolybdates. *Geochimica Cosmochimica Acta* 64, 1149-1158.
- Folk, R.L., 1968. *Petrology of sedimentary rocks*. Hemphills Austin, pp.177.
- Francoise-Elbaz-Poulichet., Pierre Sabatier., Laurent Dezileu., Remi Freydier., 2014. Sedimentary record of V, U, Mo and Mn in the Pierre-Blanche-Blanche lagoon (Southern France)- Evidence for a major anoxia event during the Roman period. *The Holocene* 24(10), 1384-1392.
- Gage, J.D., Levin, L.A., Woff, G.A., 2000. Benthic processes in the deep Arabian Sea: introduction and overview. *Deep-Sea Research II*, 47, 1-7

- Haake, B., Ittekkot, V., Ramaswamy, V., Nair, R.R., Honjo, S., 1992. Fluxes of aminoacids and hexosamines to the deep Arabian Sea. *Marine Chemistry* 40, 291-314.
- Hashimi, N.H., Nigam, R., Nair, R.R., Rajagopalan, G., 1995. Holocene Sea Level Fluctuations On Western Indian Continental Margin: An Update. *Journal Geological Society of India* 46, 157-162.
- Helz, G.R., Miller, C.V., Charnock, J.M., Mosselmans, J.F.W., Patrick, R.A.D., Gardner, C.D., Vaughan, D.J., 1996. Mechanism of molybdenum removal from the sea and concentration in black shales. EXAFS evidence. *Geochimica Cosmochimica Acta* 60, 3631-3642.
- Ingall, E.D., Bustin, R.M., Van Cappellen, P., 1993. Influence of water column anoxia on the burial and preservation of carbon and phosphorus in marine shales. *Geochimica Cosmochimica Acta* 57, 303-316.
- Invanchiko, T.S., Pedersen, T.F., 2004. Determining the influences of late Quaternary ventilation and productivity variations on Santa Barbara Basin sedimentary oxygenation: a multi-proxy approach. *Quaternary Science Reviews* 23, 467-480.
- Klinkhammer, G.P., Palmer, M.R., 1991. Uranium in the oceans: where it goes and why ?. *Geochimica Cosmochimica Acta* 55, 1799-1806.
- Kubuwara, J.S., van Geen, A., McCorkle, D.C., Bernhard, J.M., 1999. Dissolved sulfide distributions in the water column and sediment pore waters of the Santa Barbara basin. *Geochimica Cosmochimica Acta* 63, 2199-2209.
- Landing, W.M., Bruland, K.W., 1987. The contrasting biogeochemistry of iron and manganese in the Pacific Ocean. *Geochimica Cosmochimica Acta*. 51, 29-43.
- Law, G.T.W., Shimmield, T.M., Shimmield, G.B., Cowie, G.L., Breuer, E.R., Harvey, S.M., 2009. Manganese, iron, and sulfur cycling on the Pakistan margin. *Deep-Sea Research II* 56, 305-323.
- Luckge, A., Deplazes, G., Schulz, H., Scheeder, G., Suckow, A., Kasten, S., Hang, G.H., 2012. Impact of Indus River discharge on productivity and preservation of organic carbon in the Arabian Sea over the twentieth century. *Geology* 40 (5), 399-402.
- Lynne, E. C., Bonatti, D., 1965. Mobility of manganese in diagenesis of deep-sea sediments. *Marine Geology* 3, 457-474.
- Mangini, A., 1978. Th and U isotope analyses on meteor core 12310 north west African continental wise. *Meteor-Forschungsergeb Reihe C*. 29, 1-5.
- McKay, J.L., Pedersen, T.F., Southon, J., 2005. Intensification of the oxygen minimum zone in the northeast Pacific off Vancouver Island during the last deglaciation: Ventilation and/or export productivity. *Paleoceanography* 20(4), doi:10.1029/2003PA000979.
- McManus, J., Berelson, W.M., Severmann, S., Poulson, R.L., Hammond, D.E., Klinkhammer, G.P., Holm, C., 2006. Molybdenum and uranium geochemistry in continental margin sediments: paleoproxy potential. *Geochimica Cosmochimica Acta*. 70, 4646-4662.

- Mishra, S., 2000. Understanding the response of the monsoon rivers to changing climate. PAGES Workshop on South Asian Palaeoenvironments (Abstract), 44-46.
- Nair, R.R., Ittekkot, V., Manganini, S.J., Ramaswamy, V., Haake, B., Degens, E.T., Desai, B.N., Honjo, S., 1989. Increased particle flux to the deep ocean related to monsoons. *Nature* 338, 749-751.
- Nameroff, T. J., Calvert, S.E., Murray, J.W., 2004. Glacial-interglacial variability in the eastern tropical North Pacific oxygen minimum zone recorded by redox-sensitive trace metals, *Paleoceanography* 19, PA1010, doi:10.1029/2003PA000912.
- Nath, B.N., Bau, M., Rao, B.R., Rao, Ch. M., 1997. Trace and rare earth elemental variations in Arabian Sea sediments through a transect across the oxygen minimum zone. *Geochimica Cosmochim Acta*. 61, 2375-2388.
- Naqvi, W.A., 1991. Geographical extent of denitrification in the Arabian Sea in relation to some physical processes. *Oceanologica Acta* 14 (3), 281-290.
- Owens, N.J.P., Law, C.S., Mantoura, R.F.C., Burkill, P.H., Llewellyn, C.A. 1991. Methane flux to the atmosphere from the Arabian Sea. *Nature* 354, 293-296.
- Pailler, D., Bard, E., Rostek, F., Zheng, Y., Mortlock, R and van Geen, A., 2002. Burial of redox-sensitive metals and organic matter in the equatorial Indian Ocean linked to precession. *Geochimica Cosmochimica Acta* 66 (5), 849-865.
- Passier, H.F., Luther, G.W., deLange, G.J., 1997. Early diagenesis and sulphur speciation in sediments of the Oman margin, northwestern Arabian Sea. *Deep Sea Part II Tropical Studies in Oceanography* 44(6-7), 1361-1380.
- Pattan, J.N., Pearce, N.J.G., 2009. Bottom water oxygenation history in southeastern Arabian Sea during the past 140 ka: Results from redox-sensitive elements. *Palaeogeography Palaeoclimatology Palaeoecology* 280, 396-405.
- Pattan, J.N., Parthiban, G., Gupta, S.M., Ishfaq, A.M., 2012. Fe speciation and Fe/Al ratio in the sediments of southeastern Arabian Sea as an indicator of climate change. *Quaternary International* 250, 19-26
- Pattan, J.N., Partibhan, G., Anita Garg, Cesar Moraes, N.R., 2017. Intense reducing conditions during the last deglaciation and Heinrich events (H1, H2, H3) in sediments from the oxygen minimum zone off Goa, eastern Arabian Sea. *Marine and Petroleum Geology* 85, 243-256.
- Pichevin, L.E., Bard, E., Martinez, P., Billy, I. 2007. Evidence of ventilation changes in the Arabian Sea during the late Quaternary: Implication for denitrification and nitrous oxide emission. *Global Biogeochemical Cycles*. 21, GB4008.
- Qasim, S.Z. 1982. Oceanography of the northern Arabian Sea. *Deep-Sea Research* 29A, 1041-1068.
- Ramaswamy, V, Nair, R.R. 1994. Fluxes of material in the Arabian Sea and Bay of Bengal – Sediment trap studies. *Proc. Indian Acad. Sci. (Earth Planet Sci)* 103 (2), 189-210.

- Reichart, Gert-Jan., Nortier, J., Versteegh, G., Zachariasse, W.J., 2002. Periodical breakdown of the Arabian sea oxygen minimum zone caused by deep convective mixing. Geological society, London, Special Publications 195, 407-419. <https://doi.org/10.1144/GSL.SP.2002.195.01.22>
- Reichart, Gert-Jan., Brinkhuis, H., Huiskamp, F., . Zachariasse, W.J.2004. Hyperstratification following glacial overturning events in the northern Arabian Sea. *Paleoceanography* 19, PA2013.
- Rosenthal, Y., Lam, P., Boyle, E.A., Thomson, J., 1995. Authigenic cadmium enrichments in suboxic sediments: Precipitation and post depositional mobility. *Earth and Planetary Science Letters* 132, 99-111.
- Salvatteci, R., Gutierrez, D., Sifeddine, A., Ortlieb, L., Druffel, E., Boussafir, M., Schneider, R. 2016. Centennial to millennial-scale changes in oxygenation and productivity in the Eastern Tropical South Pacific during the last 25, 000 years. *Chemical Geology* 1341, 102-117.
- Sarkar, S., Bhattacharya, S.K., Sarin, M.M.,1993. Geochemical evidence for anoxic deep water in the Arabian Sea during the last deglaciation. *Geochimica Cosmochimica Acta* 57, 1009-1016.
- Scholz, F., Hensen, C.X., Noffke, A., Liebetrau, V., Wallmann, K., 2011. Early diagenesis of redox-sensitive trace metals in the Peru upwelling area: response to ENSO-related oxygen fluctuations in the water column. *Geochimica Cosmochimica Acta* 75, 7257-7276.
- Shimmield, G.B., Price N.B., 1986. The behavior of molybdenum and manganese during early sediment diagenesis- Offshore Baja California, Mexico. *Marine Chemistry* 19, 216-280.
- Shimmield, G.B., 1992. Can sediment geochemistry record changes in coastal upwelling palaeoproductivity ? Evidence from northwest Africa and the Arabian Sea. In : *Upwelling Systems: Evolution Since the Early Miocene* (eds. C.P.Summerhayes et al.) 64, 29-46.
- Sirocko, F., 1995. Abrupt change in monsoonal climate: Evidence from the geochemical composition of Arabian Sea sediments. Habilitation thesis, University of keel.
- Sukumar, R., Ramesh, R., Pant, R.K., Rajagopalan. G., 1993. A  $\delta^{13}\text{C}$  record of late Quaternary climate change from tropical peats in southern India. *Nature* 364, 703-706.
- Suthhof, A., Ittekkot, V., Gaye0Haake, B., 2001. Millennial oscillation of denitrification intensity in the Arabian Sea during Quaternary and its potential influence on atmospheric  $\text{N}_2\text{O}$  and climate. *Global Biogeochemical Cycles* 15(3), 637-649.
- Taylor, S.R., McLennan, S.M. 1985. *The continental crust: Its composition and Evolution.* Blackwell, Oxford. pp-312.
- Thamban, M., Rao, V.P., Schneider, R.R., Grootes, P.M., 2001. Glacial to Holocene fluctuations in hydrography and productivity along the southwestern continental margin of India. *Palaeogeography Palaeoclimatology Palaeoecology* 165, 113-127
- Thamban, M., Rao, V. P., Schneider, R.R., 2002. Reconstruction of late Quaternary monsoon oscillations based on clay mineral proxies using sediment core from the western margin of India. *Marine Geology* 186, 527-539.



- Tribovillard, N., Algeo, T. J., Baudin, F., Riboulleau, A., 2012. Analysis of marine environmental conditions based on molybdenum-uranium covariation-Applications to Mesozoic paleoceanography. *Chemical Geology* 324-325, 46-58.
- Tribovillard, N., Algeo, T. J., Lyons, T.W. , Riboulleaus, A., 2006. Trace metal as paleo-redox and paleo-productivity proxies: an update. *Chemical Geology* 30, 12-32.
- Tribovillard, N., Lyons, T.W., Riboulleaus, A., Bout-Roumazelles, V., 2008. A possible capture of molybdenum during early diagenesis of dysoxic sediments. *Bulletin de la Societe Geologique de France* 179(1), 3-12.
- Tribovillard, N., Ramdani, A., Trentesaux, A., 2005. Controls on organic accumulation in upper Jurassic shales of northwestern Europe as inferred from trace metal geochemistry. In: Harris (Ed). *The deposition of organic-carbon-rich sediments; models, mechanisms and consequences: Society for Sedimentary Geology Special Publication* 82, 145-162.
- Van der Weijden, C.H., Reichart, Gert-Jan., Visser Hendrik Jan., 1999. Enhanced preservation of organic matter in sediments deposited within the oxygen minimum zone in the northeastern Arabian Sea. *Deep-Sea Research I* 46, 807-830.
- Van der Weijden, C.H., Reichart, Gert-Jan., van Os, B.,J.H., 2006. Sedimentary trace element records over the last 200 kyr from within and below the northern Arabian Sea oxygen minimum zone. *Marine Geology* 231, 69-88.
- Van Geen, A, McCorkle, D.C., Klinkhammer, G.P., 1995. Sensitivity of the phosphate-cadmium-carbon isotope relation in the ocean to cadmium removal by suboxic sediments. *Paleoceanography* 10, 159-169.
- Wignall, P.B., 1994. *Black shales*. Clarendon Press, Oxford. pp-127.
- Wyrski, K., 1973. Physical Ocenaography of the Indian Ocean. *The Biology of the Indian Ocean*, G. Zeitschel and S.A. Gerlach, (Eds.), Springer Verlag, Berlin, 18-36.
- Zheng, Y., Anderson, R.F., van Gen, A., Kuwabara, J., 2000. Authigenic molybdenum formation in marine sediments: a link to pore water sulfide in the Santa Barbara basin. *Geochimica Cosmochimica Acta* 64 (24), 4165-4178.

## Captions to the figures

Figure 1. Map showing location of AAS-VI/GC-05 sediment core from the southeastern Arabian Sea (Fig. 1a). The sediment cores AAS-VI/GC-01R and AAS-VI/GC-03 studied earlier were also shown in the figure (Pattan et al. 2017). The Oxygen Minimum Zone (OMZ) covers water depth between 150 m to 1,250 m (yellow colour shaded area). The bathymetry of sediment core location ( ) is enlarged in the inset (Figure★ 1b). Holocene Sea level curve (Hashimi et al. 1995) for the western continental margin of India is shown in Figure 1c.

Figure 2. Age-depth model based on AMS dates (Fig. 2a) (Thamban et. al. 2001), sedimentation rate (Fig. 2b), dry bulk density (Fig. 2c) and bulk accumulation rate (Figure 2d) data figures for the sediment core.

Figure 3. Distribution of grain size (Fig. 3a) (Thamban et al. 2001), Ti (%) and its flux (Fig. 3b), and TOC and  $C_{org}$ : P Molar ratio (Fig. 3c) in the sediment core.

Figure 4. Distribution of productivity proxies  $CaCO_3$  and its flux (Figure 4a), TOC and its flux (Fig. 4b), P and its flux (Fig. 4c) in the sediment core during the last 18 kyr.

Figure 5. Distribution of Mn/Al & Mn flux (Fig. 5a), Fe/Al & Fe flux (Fig. 5b), Mo/Al & Mo flux (Fig. 5c), U/Th & U flux (Fig. 5d), and Cd/Al & Cd flux (Fig. 5e) in the sediment core.

Figure 6. Scatter plots of TOC versus U & Mo (Fig. 6a & 6b) in the sediment core.

Figure 7. Behaviour of U & Mo –EFs in the sediment core.

Figure 8. Authigenic Mo/U -EF distribution in the sediment core (Fig. 8a) as a proxy to infer suboxic from sulfidic conditions. The discontinuous line indicates value of 3.2 (Algeo and Tribovillard 2019) which corresponds the Mo/U –EF of Sea water (SW). Values > 3.2 indicate sulfidic conditions. Scatter plot of Mo -EF versus U -EF (Fig. 8b). The dashed lines indicate the relative proportion of Mo and U in SW  $(Mo)_{sw}/(U)_{sw} = 3.2$ ) and to fractions thereof (0.3 X SW Mo/U -EF and 3 X SW Mo/U -EF). Figure b is adopted from Tribovillard et al., 2012.

Figure 1.

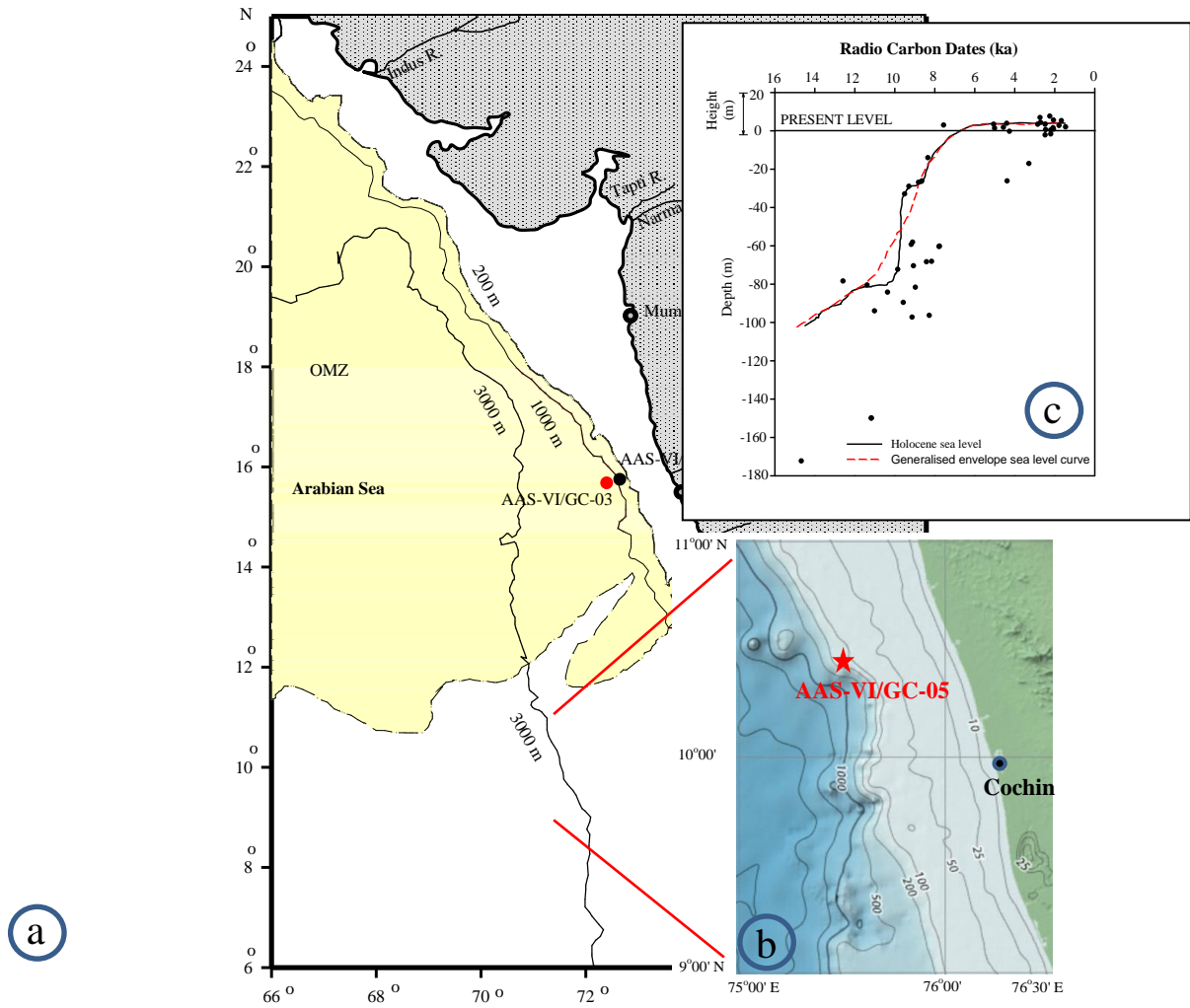


Figure 2.

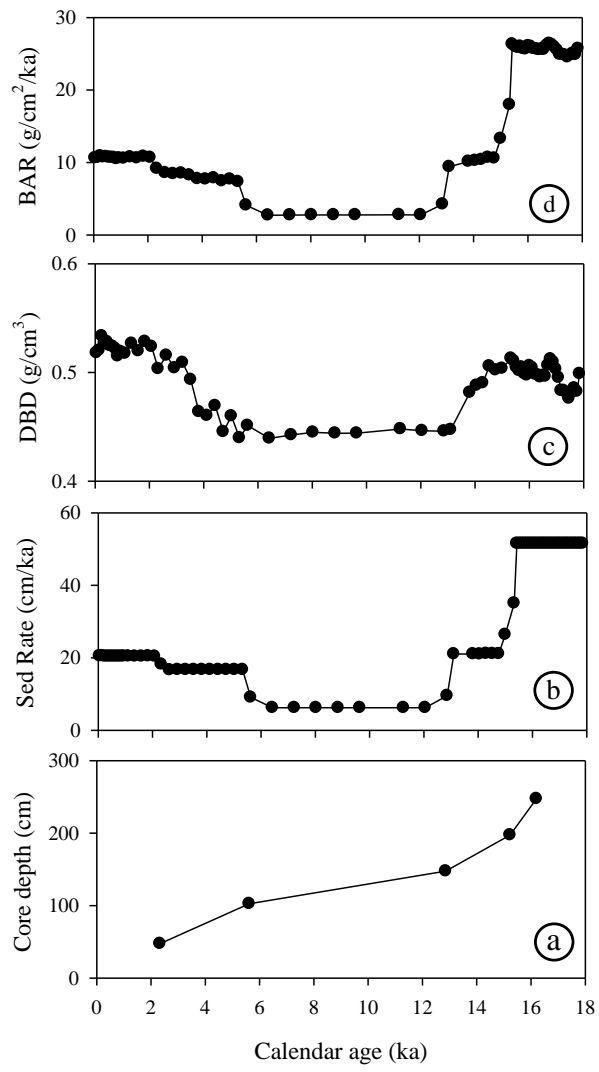


Figure 3.

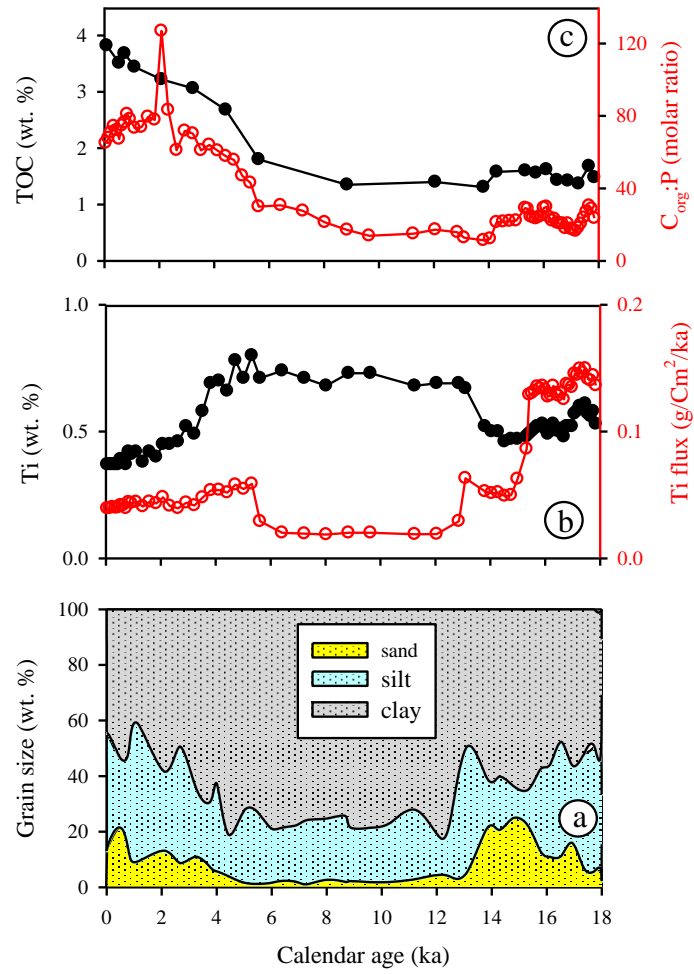


Figure 4.

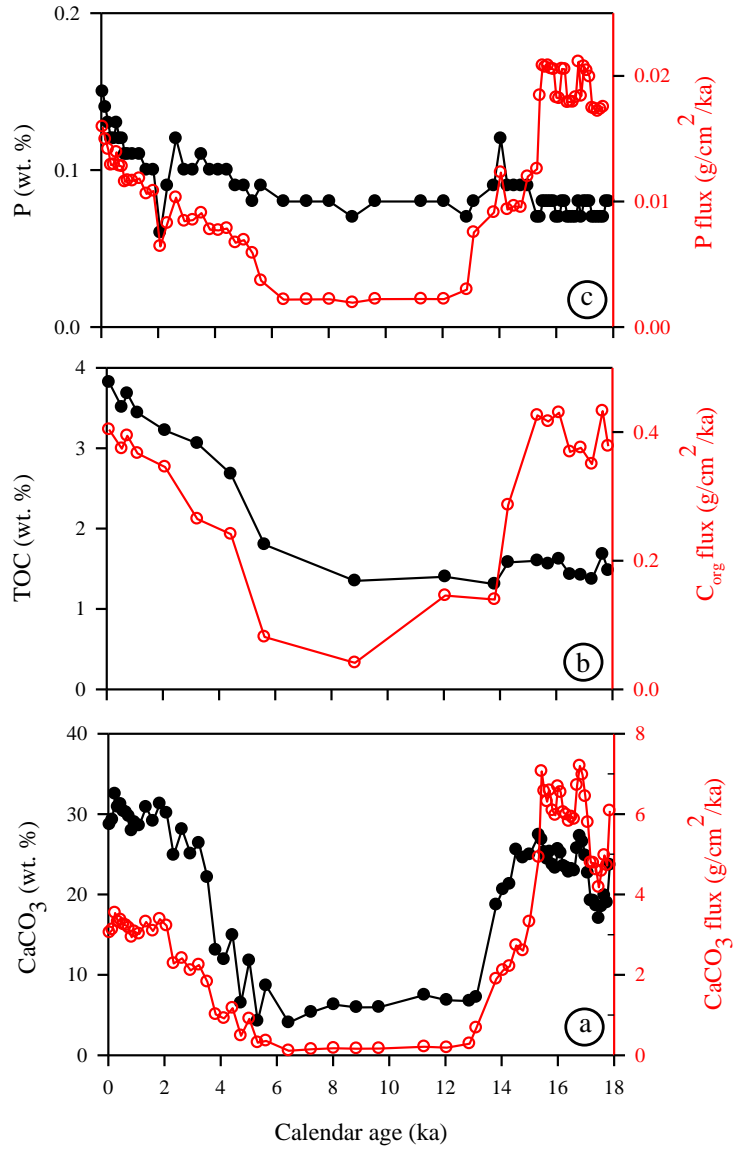


Figure 5.

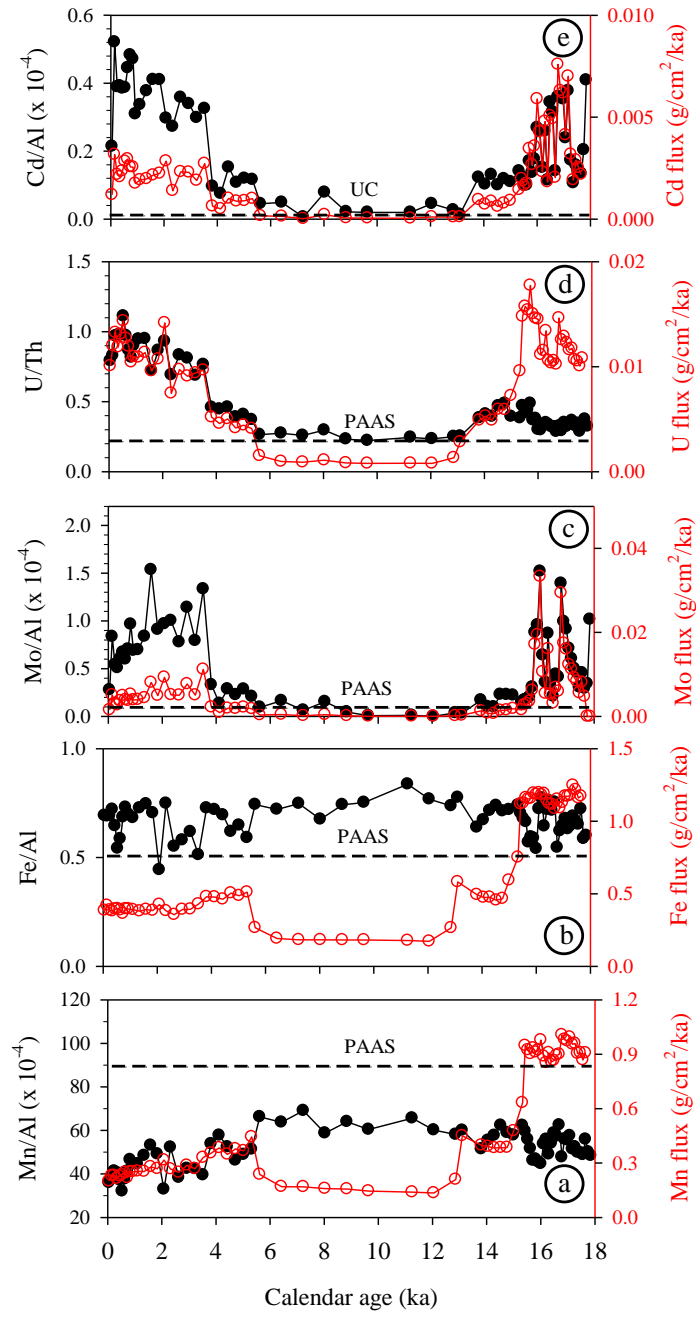


Figure 6.

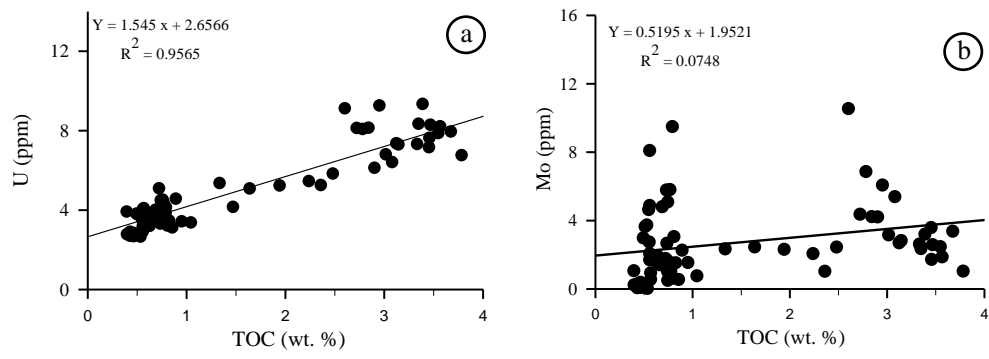




Figure 7.

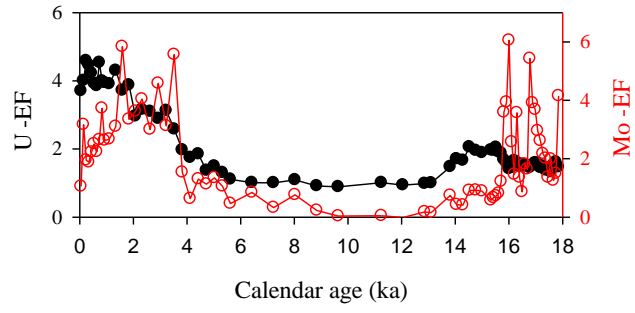


Figure 8.

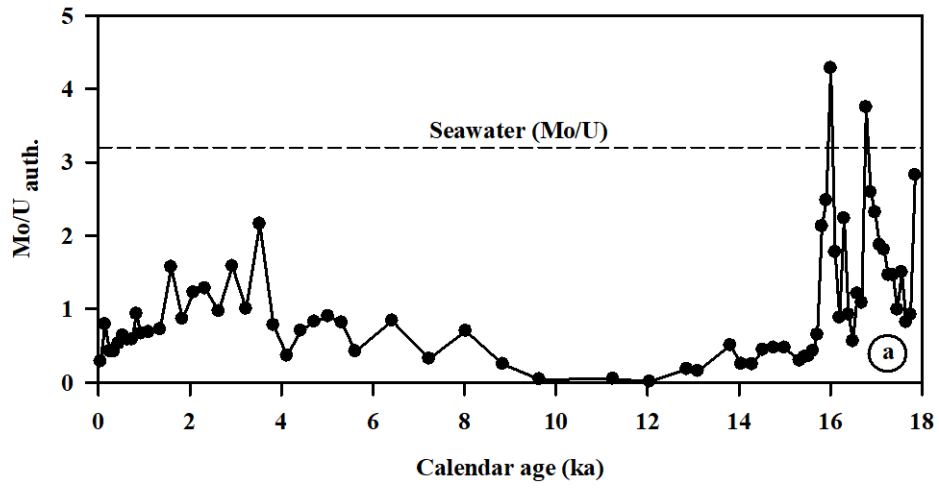
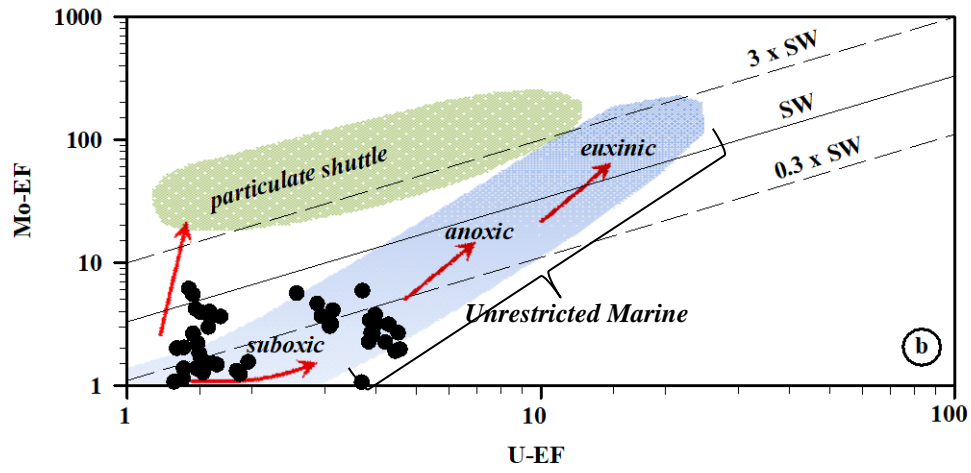


Table 1. Correlation matrix ( r ) of redox –sensitive elements (Mo, Cd and U) and productivity proxies (CaCO<sub>3</sub>, TOC and P) from a sediment core in the southeastern Arabian Sea during the last 18 kyr [p(a) < 0.01, n = 70].

	CaCO <sub>3</sub>	TOC	P	Mo	Cd	U
CaCO <sub>3</sub>	1.00					
TOC	0.50	1.00				
P	0.41	0.82	1.00			
Mo	0.38	0.23	0.04	1.00		
Cd	0.55	0.48	0.33	0.77	1.00	
U	0.57	0.93	0.75	0.40	0.61	1.00